pp 435–456. © Royal Aeronautical Society 2016
doi: 10.1017/aer.2016.4

Dispersion reduction of artillery rockets guided by flight path steering method

S. Mandić*
msmanda@open.telekom.rs
Rockets Department
Military Technical Institute
Belgrade
Serbia

ABSTRACT

Artillery rockets are sensitive to disturbances (total impulse variation, wind, thrust misalignment, etc.). As the range of ground-to-ground rockets increases, the accuracy of free flight rockets decreases. Requirements for the increase of the range and minimisation of the impact point dispersions can be solved by adding guidance and control systems to rockets. Based on the differences between the measured flight parameters and the calculated parameters for the nominal trajectory, the flight path angle correction algorithm is obtained by adding the correction to the nominal value. The flight path steering guidance system with lateral acceleration autopilot in the inner loop, is used for the guidance of hypothetical artillery rockets. The guidance algorithm given in this paper eliminates the time correction due to rocket velocity variations. Efficiency of the proposed algorithm is illustrated by numerical simulation. There is no practical influence of the external disturbances on impact point dispersion. It is also shown that the measurement errors of the inertial measurement unit are the dominant factor affecting impact point dispersion of artillery rockets modified by adding a guidance system based on the flight path steering method.

Keywords: Flight control; flight simulation; unmanned air vehicle (UAV); guided artillery rockets; simulation; missile guidance; strap-down inertial navigation system (SDINS)

* Research Engineer, Missile dynamics.

Received 29 March 2014; revised 26 January 2015; accepted 10 September 2015.

https://doi.org/10.1017/aer.2016.4 Published online by Cambridge University Press

NOMENCLATURE

$\mathbf{r}$	vector of the rocket position
$\mathbf{v}$	rocket velocity
$\mathbf{\Gamma}$	flight path angle
$\mathbf{r}_T$	vector of the target position
$x_T,\ y_T,\ h_T$	coordinates of the target
$x_i,\ y_i,\ h_i, V_i$	nominal trajectory coordinates and velocity at the sampling intervals
$x(\hat{x}_i),\ y(\hat{x}_i)$ $h(\hat{x}_i), V(\hat{x}_i)$	nominal trajectory coordinates and velocity at the estimated down range position
$\gamma_i,\ \chi_i$	nominal trajectory flight path angles at the sampling intervals
$\gamma_c,\ \chi_c$	correlated (demanded) flight path angles
$\gamma(\hat{x}_i),\ \chi(\hat{x}_i)$	nominal trajectory flight path angles at the estimated down range position
$\frac{\partial \mathbf{r}}{\partial \mathbf{r}_i}$	partial derivatives of the rocket range relative to the rocket position
$\frac{\partial \mathbf{r}}{\partial \mathbf{v}_i}$	partial derivatives of the rocket range relative to the rocket velocity
$\frac{\partial \mathbf{r}}{\partial \mathbf{\Gamma}_c}$	partial derivatives of the rocket range relative to the rocket flight path angles
$\frac{\partial \mathbf{r}}{\partial t_i}$	partial derivatives of the rocket range relative to the time
$\Delta\mathbf{r}_i$	difference between the rocket actual position and the position on the nominal trajectory
$\Delta\mathbf{v}_i$	difference between the rocket actual velocity and the nominal velocity
$\Delta\mathbf{\Gamma}_c$	difference between the rocket required flight path angle and the nominal flight path angles
Δt_i	error in time measurements
$\frac{\partial \mathbf{\Gamma}_c}{\partial \mathbf{r}_i}$	partial derivatives of the rocket flight path angles relative to the rocket position
$k_\gamma(\hat{x}_i), \tau(\hat{x}_i)$	gain and time constant of the flight path steering guidance loop
$a_{zd},\ a_{yd}$	demanded normal acceleration
$a_z,\ a_y$	realised normal acceleration
$\mathbf{v}_e^n, \mathbf{v}_e^s$	kinematic velocity relative to the Earth in navigation and spherical axis system
$\mathbf{f}^n, \mathbf{f}^s, \mathbf{f}^b$	specific force in navigation, spherical and body axis system
$\boldsymbol{\omega}_{ie}^n,\ \boldsymbol{\omega}_{ie}^s$	angular rate of the Earth relative to the inertial axis system in navigation and spherical axis system
$\boldsymbol{\omega}_{en}^n$	angular rate of the navigation axis system relative to the Earth in navigation axis system
$\boldsymbol{\omega}_{es}^s$	angular rate of the spherical axis system relative to the Earth in spherical axis system
$\boldsymbol{\omega}_{ie}^e$	angular rate of the Earth relative to the inertial axis system in Earth axis system
$\boldsymbol{\omega}_{sb}^b$	angular rate of the body relative to spherical axis system
$(\boldsymbol{\omega}_{sb}^b\times)$	skew-symmetric matrix
$\boldsymbol{\omega}_{ib}^b$	angular rate of the body relative to the inertial axis system in body axis system
$\boldsymbol{\omega}_{0s}^s$	angular rate of the spherical axis system relative to the basic axis system in body axis system
Ω	angular rate of the Earth

https://doi.org/10.1017/aer.2016.4 Published online by Cambridge University Press

$\mathbf{C}_e^s$	transformation matrix from Earth axis system to spherical axis system
$\mathbf{C}_b^s(\psi, \theta, \phi)$	transformation matrix from body to spherical axis system
$\mathbf{g}^s$	gravity acceleration matrix in spherical axis system
$\mathbf{g}_l^n,\ \mathbf{g}_l^s$	gravity in navigation and spherical axis system
$g(h),\ g_0(\varphi)$	gravity acceleration in function of altitude and on Earth's surface
A_0	azimuth of the base axis system
$\sigma_y,\ \sigma_x$	range and deviation angles in spherical axis system
$v_{x_s}, v_{y_s}, v_{z_s}$	components of kinematic velocity in spherical axis system
h	altitude
φ	latitude
x, y, h	coordinate of missile position in spherical axis system
R_0	radius of the Earth
$\mathbf{f}_{\text{acc}}$	specific force matrix measured by accelerometers
$\boldsymbol{\omega}_{\text{r.g}}$	angular rates matrix measured by rate gyros
$\mathbf{S}$	scale factor
$\mathbf{B}$	residual fixed bias
$\mathbf{n}$	random bias error
$\mathbf{w}$	noise
$N(a_{sr}, \sigma(a))$	normal Gaussian distribution low
F_N	nominal thrust
$\sigma(F)$	standard deviation of thrust
ε_F	thrust eccentricity
$\sigma(\varepsilon_F)$	standard deviation of thrust eccentricity
σ_w	standard deviation of wind

1.0 INTRODUCTION

One of the basic requirements for the direct and indirect fire of projectile and rockets is increase of the range. However, as the range of a projectile or rocket increases the delivery accuracy deteriorates. A number of disturbances can cause rounds of the direct and indirect fire of projectile to miss an intended target. These disturbances include manufacturing inaccuracies of the gun tube, launcher, propellant and projectile, atmospheric condition, firing platform motion and aiming errors. Influences of some disturbances, such as thrust misalignments and asymmetric aerodynamic, are minimised by the rocket's spinning. However, wind, total impulse variations, launcher interactions, drag and atmospheric density variations still have a significant influence on the impact points accuracy[1].

Reduction of the dispersion is achieved by adding a relatively inexpensive flight control system based on low-cost, small, rugged, micro-electromechanical sensors. There are two types of the control systems. One design concept is based on a lateral pulse jets system, and the second one is related to a set of controllable canards. Both control systems are located near the nose of the projectile. A control system requires an efficient guidance algorithm, which is usually based on estimated parameters of the projectile trajectory. An inertial navigation system (INS), which is composed of an inertial measurement unit (IMU) and a strap-down navigation algorithm, is usually used for trajectory estimation. The inertial measurement unit is composed of micro-electromechanical gyros and accelerometers fixed to the IMU body.

The US Extended Range Multiple Launch Rocket System (MLRS) program was initiated to increase the range of the rocket from 32 km to 45 km. The circular error probable (CEP)

https://doi.org/10.1017/aer.2016.4 Published online by Cambridge University Press

at a range of 45 km is approximately double the CEP at a range of 32 km. This increase of the dispersion requires the increase of the number of the rockets necessary to hit the target. In order to minimise the influence of disturbances on the impact accuracy, an extensive study was oriented to the development of a cost-effective guidance and control package which can be added to the rockets. The new Guided Multiple Launch Rocket System (GMLRS) with added cost-effective guidance and control package can defeat the target at ranges up to 70 km with significantly fewer rounds. The rocket guidance system consists of an IMU, four independent electro-mechanically actuated canards, a Global Position System (GPS), a thermal battery, a guidance computer and power supply electronics. The guidance of these rockets was based on the Flight Path Steering (FPS) and Instantaneous Impact Point (IIP). FPS was used until apogee with a constant rate of flight path angle. At apogee, the missile switched to IIP guidance which predicts the point of impact. The warhead with a guidance and control system was joined to the motor section by a roll bearing. Roll decoupling of the forward section was required to maintain roll control of the guidance section in order to enable accurate inertial navigation[2].

Analysis of the possibilities to use a lateral pulse jet control for dispersion improvement has been investigated by Harkins and Brown[3]. The set of lateral pulse jets was used to eliminate the lateral angular rate of the projectile just after the projectile left the launcher. Dispersion reduction of a direct fire rocket controlled by lateral pulse jets was analysed by Costello and Jitpraphai[4]. The six-degree-of-freedom (6DoF) mathematical model was used in projectile flight dynamic modelling. The trajectory tracking flight control system compares the measured position of the projectile with commanded trajectory to generate a position error vector in the inertial frame axis system. Position and orientation sensor feedback is assumed to be perfect, that is, not corrupted by noise, bias or cross-axis sensitivity. It was shown that dispersion reduction is a strong function of the number of pulse jets and pulse jets impulse.

Impact point dispersion of the artillery rockets with pulse jets control system was studied by Pavkovic[5]. Reference ballistic trajectory of the artillery rockets was calculated before start of the launching sequence, taking into account measured atmospheric parameters (pressure, temperature and wind). Guidance signal was based on differences between actual and reference trajectory. Optimisation of the control logic was done in order to obtain a satisfactory performance with the minimum number and intensity of control pulses. It was assumed that the estimation of the rocket position was obtained by strap-down inertial navigation system. Measurements of the accelerometers and rate gyros were assumed to be perfect without noise, bias and cross-axis sensitivity. There was no analysis of the strap-down navigation algorithm and analysis of the influence of the measurement errors to the trajectory estimation.

The pulse jet control scheme is inherently discontinuous and can be only applied at a discrete number of points, and there is also limitation in the number of the impulses. Canard control is continuous and can be applied for the full flight duration. This type of the control can provide better accuracy and reduction of impact point dispersion.

Model predictive control of a direct fire projectile equipped with canards was investigated by Ollerenshaw[6]. The projectile configuration considered in the paper is fin stabilised and the fins are slightly canted to provide moderate roll rates during flight. The control law uses an approximate closed-form solution of projectile motion to predict the states of the projectile over a set of distances, known as the prediction horizon. Control of the projectile is based on minimising the estimated error of future states. It is assumed that sensor feedback is provided by an onboard IMU.

https://doi.org/10.1017/aer.2016.4 Published online by Cambridge University Press

One of the published GMLRS guidance laws is based on the idea that the control system eliminates the differences between measured and prescribed values of the velocity vector angles and of the accelerations in the lateral directions of the rocket[7]. The prescribed values are obtained from the calculation of the nominal trajectory for a required range. In order to alleviate influence of total impulse deviation for the rockets with no thrust-termination mechanism, the correction of the prescribed flight path angle is defined empirically by trial and error. The proposed guidance law is not efficient because it is necessary to know disturbances in advance in order to determine the correction of the flight path angle in function of time.

The correlated velocity and velocity-to-be-gained guidance concept of the ballistic missile was analysed in detail by Siouris[8]. Correlated velocity is determined from a known target position and estimated missile position by a strap-down inertial navigation system. The difference between correlated and missile velocity defines velocity-to-be-gained which is used to control the missile. One type of this guidance system is *Q guidance,* which is based on *Q matrix* whose elements consist of directional derivatives. *Velocity to be gained* is determined by integration of the Q matrix in the feedback. This guidance system requires missile engine cut-off when the missile velocity becomes equal to the correlated velocity.

All guidance systems of the guided artillery rockets and ballistic missiles are based on the estimated parameters of the actual trajectory. Estimation of the trajectory is based on a strap-down navigation system and GPS receivers. The strap-down navigation system is composed of IMU and the navigation algorithm[9,10]. The mathematical model of IMU accelerometers and rate gyros measurements errors include scale factor error, bias and noise.

The purpose of this paper is to develop a flight path steering algorithm for artillery rockets whose entire trajectory is in dense layers of atmosphere. The task of the guidance law is to minimise the influence of the atmospheric disturbances and thrust eccentricity without possibility to control the magnitude of the velocity by solid rocket motor burn-out.

The published guidance laws for the artillery rockets are based on the spatial distance between real and reference trajectory.

Beside compensation of deviation of real from reference trajectory in the plane normal to the trajectory, the advance of flight path steering guidance law, developed in the paper, also includes compensation of the rocket velocity deviation from nominal values. The desired flight path angle is a linear function of these deviations and sensitive coefficients estimated before rocket flight by calculation of the miss distance at the impact points due to variation of the flight parameters.

A strap-down inertial navigation algorithm will be used for estimation of missile velocity, flight path angle and missile position in space. Estimation of the missile trajectory parameters depends on the navigation algorithm and IMU accuracy. Efficiency of the guidance algorithm can be verified by numerical simulation of the missile flight, guidance and control systems, navigation algorithm and IMU measurement errors. Numerical simulation results show that the proposed guidance algorithm will correct deviations in both trajectory and velocity.

2.0 COMPENSATION OF TRAJECTORY AND VELOCITY DEVIATION BY FLIGHT PATH ANGLE

The nominal trajectory for the required range of the ground-to-ground rockets is a ballistic trajectory in the standard atmosphere without disturbances and with nominal thrust. This trajectory is obtained by the numerical simulation of the ballistic flight by using a six-degree-of-freedom (6DoF) mathematical model of the rocket in flight.

https://doi.org/10.1017/aer.2016.4 Published online by Cambridge University Press

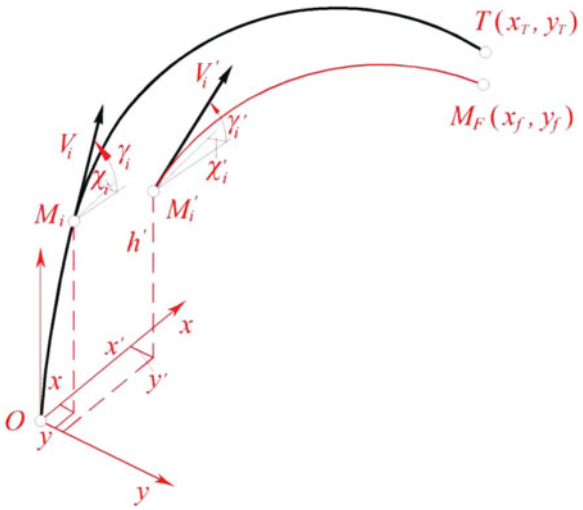


Figure 1. (Colour online) Trajectory deviation.

The deviation of the actual trajectory relative to the nominal trajectory is illustrated in Fig. 1. The position of the target on the ground is defined by the coordinates x_T and y_T.

In order to simplify the derivation of the mathematical model for the flight path angle correction, the following matrix notation will be used in the paper:

$$\mathbf{r} = \begin{bmatrix} x \\ y \\ h \end{bmatrix}, \mathbf{v} = \begin{bmatrix} V \end{bmatrix} \quad \text{and} \quad \Gamma = \begin{bmatrix} \gamma \\ \chi \end{bmatrix} \qquad \ldots (1)$$

In arbitrary time instance $t = t_i$, the position of the rocket is defined by the point M_i (Fig. 1). The ballistic flight of the rockets from the point M_i to the target is defined by the velocity V_i and the flight path angles γ_i and χ_i. This ballistic flight provides rocket impact points at the position of the target. The equality of the rocket and target position at the impact point can be written in the vector form

$$\mathbf{r}_T - \mathbf{r}_F(\mathbf{r}_i, \mathbf{v}_i, \Gamma_i, t_i) = 0, \qquad \ldots (2)$$

where t_i is the initial time for the ballistic flight from the arbitrary point; M_i, $\mathbf{r}_T = [x_T \; y_T]^T$ is the target position (for the surface target $h_T = 0$), $\mathbf{r}_F = [x_F \; y_F]^T$ is the impact point of the rocket at the end of the flight, $t = t_f$, $\mathbf{r}_i = [x_i \; y_i \; h_i]^T$ is the rocket position on the nominal trajectory in the time instance $t = t_i$, and $\Gamma_i = [\gamma_i \; \chi_i]^T$ is the flight path angles in the vertical and horizontal plane at the time instance $t = t_i$.

If the flight path angles at the initial instance of the ballistic flight are equal to the required (correlated) ones, then the rocket position at the end of the flight ($t = t_f$) will be equal to the target position.

$$\gamma_i = \gamma_c, \chi_i = \chi_c \qquad \ldots (3)$$

$$\mathbf{r}_T - \mathbf{r}(\mathbf{r}_i, \mathbf{v}_i, \Gamma_i, t_f) = 0 \qquad \ldots (4)$$

https://doi.org/10.1017/aer.2016.4 Published online by Cambridge University Press

In the case of disturbances, the rocket will not be at the point M_i on the nominal trajectory but at some point M_i' away from the nominal trajectory. The point M_i on the nominal trajectory corresponds to the time instance t_i. Since there are some errors in the measurement of the current time, the measured time t_i' corresponds to the point M_i'. The values of the flight path angles, at the time instance $t = t_i'$, can be determined from the condition that the ballistic flight of the rocket from this time instance can hit the target.

$$\gamma_i' = \gamma_c, \quad \chi_i' = \chi_c \qquad \ldots(5)$$

The correlated flight path angles at the point M_i can be defined in the matrix form $\Gamma_\mathbf{c} = [\gamma_c \ \chi_c]^T$. The general condition that a rocket with the ballistic flight from the point M_i' hits the target is defined by the equation

$$\mathbf{r}_T - \mathbf{r}_F\left(\mathbf{r}_i', \mathbf{v}_i', \Gamma_c, t_i'\right) = 0 \qquad \ldots(6)$$

The second term in Equation (6) can be developed in the Taylor's series relative to the point M_i on the nominal trajectory.

$$\begin{aligned}\mathbf{r}_T - \mathbf{r}_F\left(\mathbf{r}_i', \mathbf{v}_i', \Gamma_c, t_i'\right) &= \mathbf{r}_T - \mathbf{r}\left(\mathbf{r}_i, \mathbf{v}_i, \Gamma_i, t_f\right) \\ &- \left[\frac{\partial \mathbf{r}_F}{\partial \mathbf{r}_i}\Delta\mathbf{r}_i + \frac{\partial \mathbf{r}_F}{\partial \mathbf{v}_i}\Delta\mathbf{v}_i + \frac{\partial \mathbf{r}_F}{\partial \Gamma_i}\Delta\Gamma_c + \frac{\partial \mathbf{r}_F}{\partial t_f}\Delta t_f\right] = 0\end{aligned} \qquad \ldots(7)$$

The partial derivatives are given for the nominal trajectory parameters $\mathbf{r}(\mathbf{r}_i, \mathbf{v}_i, \Gamma_i, t_i)$.

$$\frac{\partial \mathbf{r}_F}{\partial \mathbf{r}_i} = \begin{bmatrix} \frac{\partial x_f}{\partial x_i} & \frac{\partial x_f}{\partial y_i} & \frac{\partial x_f}{\partial h_i} \\ \frac{\partial y_f}{\partial x_i} & \frac{\partial y_f}{\partial y_i} & \frac{\partial y_f}{\partial h_i} \end{bmatrix}_{\mathbf{r}_i, \mathbf{v}_i, \Gamma_i, t_i} \qquad \ldots(8)$$

$$\frac{\partial \mathbf{r}_F}{\partial \mathbf{v}_i} = \begin{bmatrix} \frac{\partial x_f}{\partial V_i} \\ \frac{\partial y_f}{\partial V_i} \end{bmatrix}_{\mathbf{r}_i, \mathbf{v}_i, \Gamma_i, t_i} \qquad \ldots(9)$$

$$\frac{\partial \mathbf{r}_F}{\partial \Gamma_c} = \begin{bmatrix} \frac{\partial x_f}{\partial \gamma_i} & \frac{\partial x_f}{\partial \chi_i} \\ \frac{\partial y_f}{\partial \gamma_i} & \frac{\partial y_f}{\partial \chi_i} \end{bmatrix}_{\mathbf{r}_i, \mathbf{v}_i, \Gamma_i, t_i} \qquad \ldots(10)$$

$$\frac{\partial \mathbf{r}_F}{\partial t_i} = \begin{bmatrix} \frac{\partial x_f}{\partial t_i} \\ \frac{\partial y_f}{\partial t_i} \end{bmatrix}_{\mathbf{r}_i, \mathbf{v}_i, \Gamma_i, t_i} \qquad \ldots(11)$$

$$\Delta\mathbf{r}_i = \mathbf{r}_i' - \mathbf{r}_i = \begin{bmatrix} x_i' - x_i \\ y_i' - y_i \\ h_i' - h_i \end{bmatrix} = \begin{bmatrix} \Delta x_i \\ \Delta y_i \\ \Delta h_i \end{bmatrix} \qquad \ldots(12)$$

$$\Delta\Gamma_i = \Gamma_i' - \Gamma_i = \begin{bmatrix} \gamma_i' - \gamma_i \\ \chi_i' - \chi_i \end{bmatrix} = \begin{bmatrix} \Delta\gamma_i \\ \Delta\chi_i \end{bmatrix} \qquad \ldots(13)$$

https://doi.org/10.1017/aer.2016.4 Published online by Cambridge University Press

$$\Delta \mathbf{v}_i = \mathbf{v}'_i - \mathbf{v}_i = \left[V'_i - V_i \right] = \left[\Delta V_i \right] \quad \ldots (14)$$

$$\mathbf{r}_T - \mathbf{r}_F \left(\mathbf{r}_i,\ \mathbf{v}_i,\ \Gamma_i, t_i \right) = 0 \quad \ldots (15)$$

Partial derivatives can be determined by the method of differential corrections. This method is related to the numerical determination of the first derivative of the trajectory coordinates relative to the parameters that define ballistic flight trajectory from the point M_i to the target.

$$\begin{aligned} \frac{\partial x_f}{\partial p_i} &= \frac{x_f \left(p_1,\ ..p_i + \Delta p_i, ..p_n \right) - x_f \left(p_1, ..p_i, ..p_n \right)}{\Delta p_i} \\ \frac{\partial y_f}{\partial p_i} &= \frac{y_f \left(p_1,\ ..p_i + \Delta p_i, ..p_n \right) - y_f \left(p_1, ..p_i, ..p_n \right)}{\Delta p_i} \end{aligned}, \quad \ldots (16)$$

where $p_1 = x$, $p_2 = y$, $p_3 = h$, $p_4 = V$, $p_5 = \gamma$, $p_6 = \chi$ and $p_7 = t$.

The increment of the flight path angles due to disturbances can be determined from Equation (7) since the first two terms, $\mathbf{r}_T$ and $\mathbf{r}_F(\mathbf{r}_i, \mathbf{v}_i,\ \Gamma_i,\ t_0)$, are equal.

$$\begin{aligned} \Delta \Gamma_c = &- \left(\frac{\partial \mathbf{r}_F}{\partial \Gamma_c} \right)^{-1} \left(\frac{\partial \mathbf{r}_F}{\partial \mathbf{r}_i} \right) \Delta \mathbf{r}_i - \left(\frac{\partial \mathbf{r}_F}{\partial \Gamma_c} \right)^{-1} \left(\frac{\partial \mathbf{r}_F}{\partial \mathbf{v}_i} \right) \Delta \mathbf{v}_i \\ &- \left(\frac{\partial \mathbf{r}_F}{\partial \Gamma_c} \right)^{-1} \left(\frac{\partial \mathbf{r}_F}{\partial t_i} \right) \Delta t_i \end{aligned} \quad \ldots (17)$$

Equation (17) can be simplified by using a new notation of the matrix:

$$\frac{\partial \Gamma_c}{\partial \mathbf{r}_i} = - \left(\frac{\partial \mathbf{r}_F}{\partial \Gamma_c} \right)^{-1} \left(\frac{\partial \mathbf{r}_F}{\partial \mathbf{r}_i} \right), \quad \ldots (18)$$

$$\frac{\partial \Gamma_c}{\partial \mathbf{v}_i} = - \left(\frac{\partial \mathbf{r}_F}{\partial \Gamma_c} \right)^{-1} \left(\frac{\partial \mathbf{r}_F}{\partial \mathbf{v}_i} \right) \text{ and} \quad \ldots (19)$$

$$\frac{\partial \Gamma_c}{\partial t_i} = - \left(\frac{\partial \mathbf{r}_F}{\partial \Gamma_c} \right)^{-1} \left(\frac{\partial \mathbf{r}_F}{\partial t_i} \right) \quad \ldots (20)$$

Substituting Equations (18), (19) and (20) into Equation (17) the relation between the flight path angles increment $\Delta \Gamma_c$ and disturbances $\Delta \mathbf{r}_i$, $\Delta \mathbf{v}_i$, Δt_i can be written in a simplified form:

$$\Delta \Gamma_c = - \left(\frac{\partial \Gamma_c}{\partial \mathbf{r}_i} \right) \Delta \mathbf{r}_i - \left(\frac{\partial \Gamma_c}{\partial \mathbf{v}_i} \right) \Delta \mathbf{v}_i - \left(\frac{\partial \Gamma_c}{\partial t_i} \right) \Delta t_i, \quad \ldots (21)$$

where $\Delta \Gamma_c = [\, \Delta \gamma_c \quad \Delta \chi_c \,]^T$.

In general, there are coupling effects between the disturbances in the vertical and horizontal plane and the flight path correction in these two planes. In order to analyse these

https://doi.org/10.1017/aer.2016.4 Published online by Cambridge University Press

cross-influences, the matrix Equation (21) can be written in a developed form:

$$\begin{bmatrix} \Delta\gamma_c \\ \Delta\chi_c \end{bmatrix} = -\begin{bmatrix} \frac{\partial\gamma_c}{\partial x_i} & \frac{\partial\gamma_c}{\partial y_i} & \frac{\partial\gamma_c}{\partial h_i} \\ \frac{\partial\chi_c}{\partial x_i} & \frac{\partial\chi_c}{\partial y_i} & \frac{\partial\chi_c}{\partial h_i} \end{bmatrix} \begin{bmatrix} \Delta x_i \\ \Delta y_i \\ \Delta h_i \end{bmatrix} - \\ -\begin{bmatrix} \frac{\partial\gamma_c}{\partial V_i} \\ \frac{\partial\chi_c}{\partial V_i} \end{bmatrix} \Delta V_i - \begin{bmatrix} \frac{\partial\gamma_c}{\partial t_i} \\ \frac{\partial\chi_c}{\partial t_i} \end{bmatrix} \Delta t_i \qquad \ldots (22)$$

Based on the analysis of the rocket's ballistic flight, the variation of the flight path angle in the vertical plane ($\Delta\gamma_i$) creates only the variation of the range (Δx_f); and, the variation of the flight path angle in the horizontal plane ($\Delta\chi_i$) creates only the deviation of the rocket trajectory (Δy_f).

Neglecting cross-coupling sensitive coefficients, Equation (23) can be written in the form of two separate equations. One equation gives the relation between the flight path angle increment in the vertical plane ($\Delta\gamma_c$) and disturbances Δx_i, Δh_i, ΔV_i. The second equation (Equation (24)) gives the relation between the flight path angle variation in the horizontal plane ($\Delta\chi_c$) and the displacement of the rocket relative to the nominal trajectory in the horizontal plane (Δy_i).

$$\Delta\gamma_c = -\frac{\partial\gamma_c}{\partial x_i}\Delta x_i - \frac{\partial\gamma_c}{\partial h_i}\Delta h_i - \frac{\partial\gamma_c}{\partial V_i}\Delta V_i \qquad \ldots (23)$$

$$\Delta\chi_c = -\frac{\partial\chi_c}{\partial y_i}\Delta y_i \qquad \ldots (24)$$

The total time of the rocket flight depends on the total impulse of the rocket engine. The corrective factor of the total impulse is a ratio between the actual total impulse and the nominal value of the total impulse ($K_{I_{tot}} = I_{tot}/I_{totN}$).

The diagrams of the velocities of the hypothetical rocket in function of time are given in Fig. 2 and the diagrams of the same velocities in function of the range are given in Fig. 3. There are three curves related to the three values of the corrective factors of the total impulse $K_{I_{tot}} = 1.0$, 0.96 and 1.04.

The guidance method given in the paper requires two separate calculations:

2.1 Calculation before the missile flight

The nominal trajectory parameters (x_i, y_i, h_i, V_i) and the sensitive coefficients ($\partial\gamma_c/\partial x_i$, $\partial\gamma_c/\partial h_i$, $\partial\gamma_c/\partial V_i$, $\partial\chi_c/\partial y_i$) are calculated before launching the rocket using the following procedure:

- Calculation of the nominal trajectory (ballistic trajectory without external disturbances) by a 6DoF mathematical model of the missile in flight for a given target,
- Selection of the control points on the nominal trajectory from the condition that the linear interpolation of the trajectory parameters can be applied between two successive control points,

https://doi.org/10.1017/aer.2016.4 Published online by Cambridge University Press

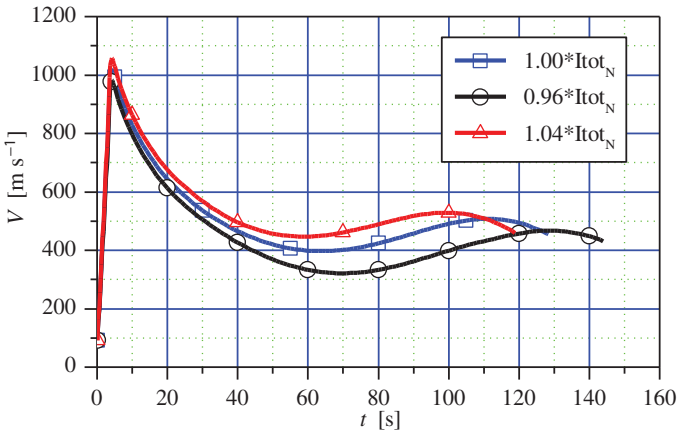


Figure 2. (Colour online) Rocket velocity in function of time.

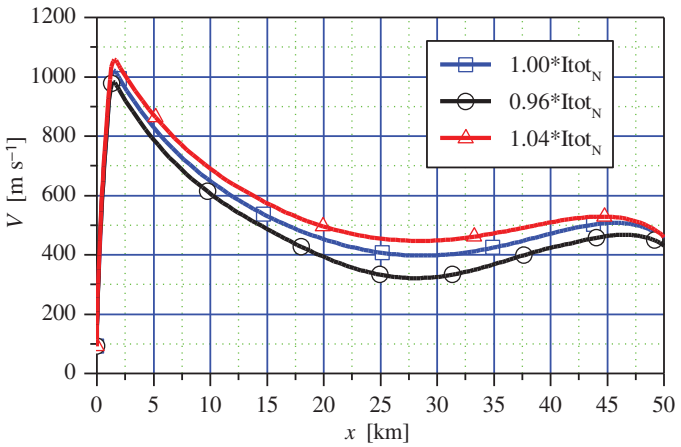


Figure 3. (Colour online) Rocket velocity as a function of range.

- Calculation of the corrective coefficients at the control points,
- Downloading of the nominal trajectory parameters and the corrective coefficients into the computer memory of rockets.

2.2 Calculation during the missile flight

- Selection of the control points based on the estimated parameters of the missile trajectory (SDINS – strap-down inertial navigation system),
- Calculation of the flight path angle correction based on the difference between the parameters of the estimated trajectory and the nominal one (23), (24),
- Calculation of the required (correlated) flight path angle by adding the flight path angle correction to the nominal value.

https://doi.org/10.1017/aer.2016.4 Published online by Cambridge University Press

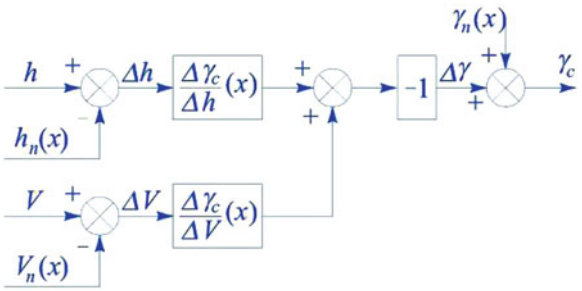


Figure 4. (Colour online) Correlated flight path angle algorithm.

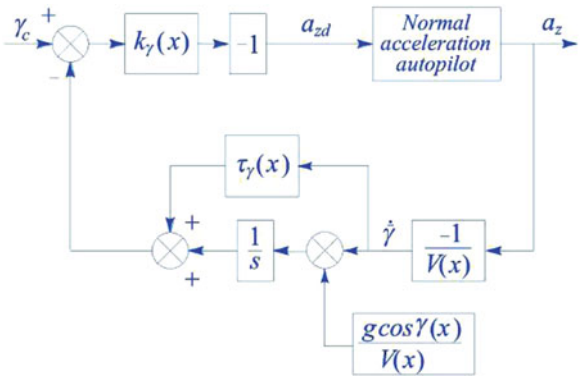


Figure 5. (Colour online) Flight path angle guidance loop.

If the nominal trajectory parameters and the sensitive coefficients are a function of the range, then the flight path angle corrections ($\Delta\gamma_c$, $\Delta\chi_c$) are also a function of the range. Consequently, the equation for the flight path correction can be written in a function of the range

$$\Delta\gamma_c(x) = -\frac{\partial\gamma_c}{\partial h}(x)\,\Delta h(x) - \frac{\partial\gamma_c}{\partial V}(x)\,\Delta V(x) \quad \ldots(25)$$

$$\Delta\chi_c(x) = -\frac{\partial\chi_c}{\partial y}(x)\,\Delta y(x) \quad \ldots(26)$$

The correlated (desired) flight path angle in the vertical plane γ_c is obtained by adding the corrections $\Delta\gamma_c$ to the nominal value of the flight path angle γ_n (Fig. 4). The nominal value of the flight path angle γ_n is obtained by linear interpolation between values of the flight path angle in two neighbouring control points i and $i+1$.

$$\gamma_c(x) = \gamma_n(x) + \Delta\gamma_c(x) \quad \ldots(27)$$

The flight path guidance loop (Fig. 5) is used to generate the demanded acceleration a_{zd} to eliminate the difference between the estimated ($\tilde{\gamma}$) and desired (γ_c) values of

https://doi.org/10.1017/aer.2016.4 Published online by Cambridge University Press

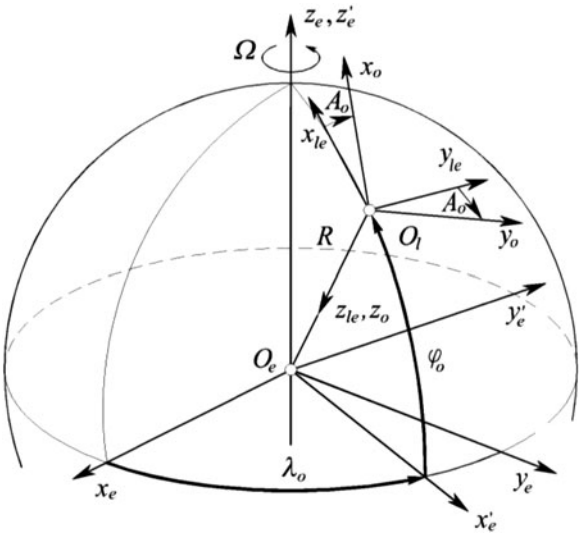


Figure 6. Basic and local Earth-fixed and basic axis system.

the flight path angle[8].

$$a_{zd} = V\, k_\gamma \left[\gamma_c - (\tilde{\gamma} + \tau_\gamma \dot{\tilde{\gamma}})\right] \quad \ldots (28)$$

The lateral (normal) acceleration autopilot consists of a major accelerometer feedback loop to control the missile's lateral acceleration, and a minor rate feedback loop which provides the necessary damping of the missile pitch or yaw rates[8,11,12]. The design procedure for determination of the autopilot gains are based on classical and digital automatic control[11-14].

3.0 MATHEMATICAL MODEL OF SDINS NAVIGATION

SDINS navigation is widely used for estimation of the rocket position and velocity. Position and velocity estimation is based on the known initial position and initial velocity, and on measured specific forces and angular rates.

The differential equation of the rocket velocity in an arbitrary navigation axis system[9] is

$$\dot{\mathbf{v}}_e^n = \mathbf{f}^n - \left[2\boldsymbol{\omega}_{ie}^n + \boldsymbol{\omega}_{en}^n\right] \times \mathbf{v}_e^n + \mathbf{g}_l^n \quad \ldots (29)$$

The position of the target relative to the launching position is defined by the basic axis system which is Earth's fixed axis system (F_0). The origin of the basic axis system coincides with the launch point. The Ox_0 axis is directed to the target. The plane Ox_0y_0 is tangent to the Earth's surface and the axis Oz_0 is directed vertically down (along the gravity vector). The position of F_0 is determined by the azimuth angle A_0 with respect to the local Earth-fixed reference frame F_{le}[10] (Fig. 6).

Since guidance of the ground-to-ground rockets requires correction of the rocket position relative to the ballistic trajectory, the spherical axis system (F_S) is used for the navigation

https://doi.org/10.1017/aer.2016.4 Published online by Cambridge University Press

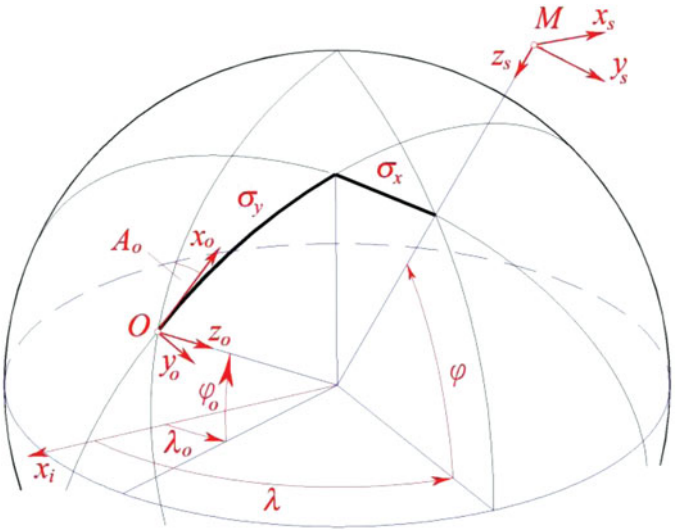


Figure 7. (Colour online) Spherical axis system.

system. Position of the spherical axis system relative to the basic axis system is defined by range angle σ_y and deviation angle σ_x (Fig. 7).

The differential equation of the kinematic velocity in arbitrary navigation can be applied to the spherical axis system.

$$\dot{\mathbf{v}}_e^s = \mathbf{f}^s - \left[2\boldsymbol{\omega}_{ie}^s + \boldsymbol{\omega}_{es}^s\right] \times \mathbf{v}_e^s + \mathbf{g}_l^s, \quad \ldots (30)$$

where $\mathbf{v}_e^s$ is kinematic velocity of the rocket in spherical axis system

$$\mathbf{v}_e^s = \left[\, v_{x_s} \;\; v_{y_s} \;\; v_{z_s} \,\right]^T \quad \ldots (31)$$

Angular rate of the Earth relative to the inertial axis system in spherical axis system ($\boldsymbol{\omega}_{ie}^s$) can be obtained by multiplication of the angular rate of the Earth in Earth axis system $\boldsymbol{\omega}_{ie}^e = [0 \quad 0 \quad \Omega]^T$ and transformation matrix from Earth axis system to spherical axis system.

$$\boldsymbol{\omega}_{ie}^s = \mathbf{C}_e^s \, \boldsymbol{\omega}_{ie}^e \quad \ldots (32)$$

Angular rate of the spherical axis system relative to the basic axis system is defined by two angular rates $\dot{\sigma}_x$ and $\dot{\sigma}_y$. These two angular rates depend on rocket velocity relative to Earth in spherical axis system v_{xS}, v_{yS} and rocket altitude h.

$$\boldsymbol{\omega}_{0s}^s = \left[\, 0 \quad \dot{\sigma}_y \quad \dot{\sigma}_x \,\right]^T = \left[\, 0 \quad \frac{v_{xS}}{R_0 + h} \quad \frac{-v_{yS}}{R_0 + h} \,\right]^T \quad \ldots (33)$$

Specific force in spherical axis system $\mathbf{f}^s$ is determined by specific force in body axis system $\mathbf{f}^b$ and transformation matrix from body to spherical axis system $\mathbf{C}_b^s(\psi, \theta, \phi)$.

$$\mathbf{f}^s = \mathbf{C}_b^s(\psi, \theta, \phi) \;\; \mathbf{f}^b \quad \ldots (34)$$

https://doi.org/10.1017/aer.2016.4 Published online by Cambridge University Press

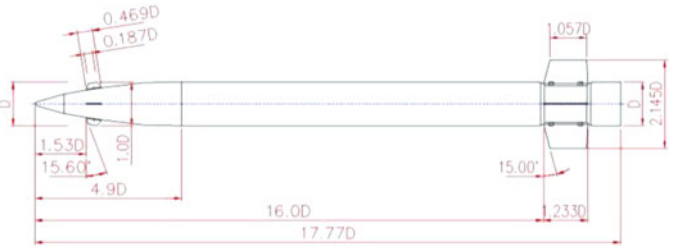


Figure 8. (Colour online) Basic dimensions of the guided artillery rocket.

Gravity has only components in the z_s direction of the spherical axis system

$$\mathbf{g}^s = \begin{bmatrix} 0 & 0 & g(h) \end{bmatrix}^T, \quad \ldots (35)$$

where $g(h)$ depends on rocket altitude (h) and the gravitational acceleration on the Earth's surface $g_0(\varphi)$.

$$g(h) = \frac{g_0(\varphi)}{(1 + h/R_0)^2}, \quad \ldots (36)$$

where φ is latitude.

The rate of change of direction cosine matrix $\dot{\mathbf{C}}_b^s$ depends on angular rate of the body relative to spherical axis system in body axis system $\boldsymbol{\omega}_{sb}^b$.

$$\dot{\mathbf{C}}_b^s = \mathbf{C}_b^s \left(\boldsymbol{\omega}_{sb}^b \times \right), \quad \ldots (37)$$

where $(\boldsymbol{\omega}_{sb}^b \times)$ is skew-symmetric matrix of $\boldsymbol{\omega}_{sb}^b$, which is a function of angular rate in body axis system $\boldsymbol{\omega}_{ib}^b$.

$$\boldsymbol{\omega}_{sb}^b = \boldsymbol{\omega}_{ib}^b - \mathbf{C}_s^b \left[\boldsymbol{\omega}_{ie}^s + \boldsymbol{\omega}_{0s}^s \right] \quad \ldots (38)$$

Position of the rocket in basic axis system is defined by the kinematic velocity of the rocket in spherical axis system.

$$\begin{bmatrix} \dot{x} & \dot{y} & \dot{h} \end{bmatrix}^T = \begin{bmatrix} \dfrac{v_{x_S}}{1 + \dfrac{h}{R_0}} & \dfrac{v_{y_S}}{1 + \dfrac{h}{R_0}} & -v_{z_S} \end{bmatrix}^T \quad \ldots (39)$$

4.0 RESULTS OF NUMERICAL SIMULATION

The basic dimensions of the artillery rocket analysed in the paper are given in Fig. 8. The total impulse of the thrust is $I_{tot} = 33400\ daNs$. There are buster and sustainer phases of the solid rocket motors. The buster phase of the rocket motor lasts for 0.8 s. The total burn out time is 4 s. The total mass of the rocket is $m_0 = 390$ kg.

In order to verify the efficiency of the flight path guidance system, a computer program for rocket flight with a complete guidance and control system has been designed. The flight path

https://doi.org/10.1017/aer.2016.4 Published online by Cambridge University Press

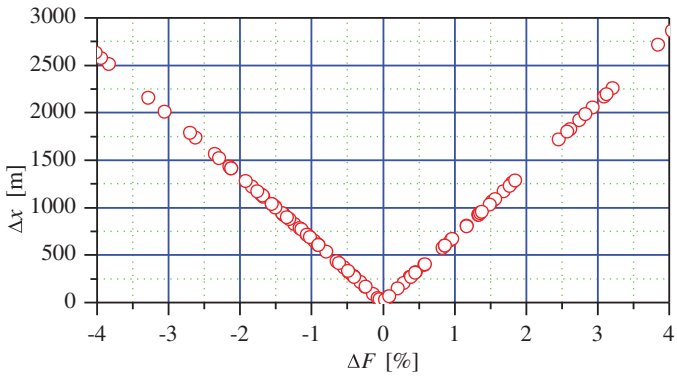


Figure 9. (Colour online) Miss distance due to total impulse deviation.

guidance system has been included in the program together with synthetic pitch autopilots with accelerometers and rate gyros.

The flight path guidance system is used to generate the demanded acceleration a_{zd} to eliminate the difference between the estimated ($\tilde{\gamma}$) and correlated (γ_c) values of the flight path angle. The synthesis of the guidance loop and the synthetic lateral autopilot is carried out by the classical theory of automatic control for a hypothetic missile with the maximum range of 50 km[11-14].

The efficiency of the proposed trajectory correction of artillery rockets is verified for the deviation of the total impulse. Since the total impulse is directly related to the thrust, the variation of the total impulse is obtained by multiplying the nominal values of the thrust with the corrective factors $K_{I_{tot}}$.

The ballistic trajectories for three values of the total impulse are given in Fig. 6. One trajectory is calculated for the nominal value of the total impulse. The other two trajectories are obtained for the thrust values 4% higher and 4% lower than the nominal ones. The corrective factors of the total impulse for these two cases are equal to $K_{I_{tot}} = 1.04$ and $K_{I_{tot}} = 0.96$. The miss distances at the impact point, due to 4% total impulse variations, are approximately 3 km. On the basis of the achieved ranges of these three ballistic trajectories, it can be concluded that the total impulse deviation has a significant influence on the range variation.

The absolute values of the miss distance as a function of the percentage of the total impulse deviation for the ballistic flight of the rockets are given in Fig. 9. This diagram is obtained by the Monte Carlo simulation. One hundred runs have been performed with the standard deviation of the thrust of $\sigma_F = 2.0\%$.

The trajectories of the rockets guided by the flight path steering guidance are given in Fig. 10. There are three trajectories (Fig. 10) related to the variation of the total impulse ($K_{I_{tot}}$ =1.0, 0.96 and 1.04). After the ballistic flight in the first phase, one second after the launch, the guidance with a trajectory correction starts. In all the analyses, the rocket is guided to the end of the flight (impact into a surface).

When the total impulse is higher than the nominal total impulse, the flight path correction formula (Equation (26)) decreases the flight path angle relative to the nominal flight path angle and the trajectory is below the nominal trajectory. When the total impulse is lower than the nominal one, the required flight path angle is greater than the nominal one and the trajectory is above the nominal one.

https://doi.org/10.1017/aer.2016.4 Published online by Cambridge University Press

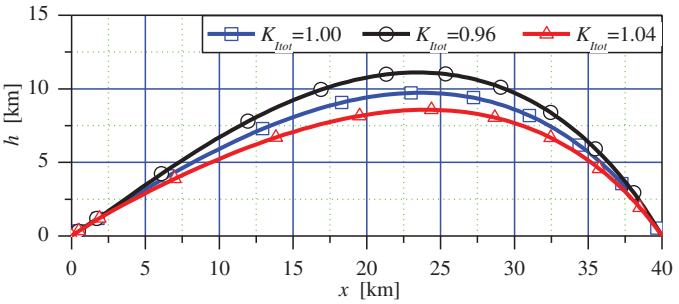


Figure 10. (Colour online) Influence of the total impulse variation on the guided rocket range.

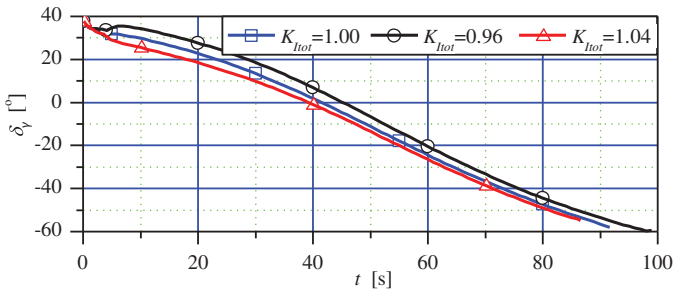


Figure 11. (Colour online) Flight path angle.

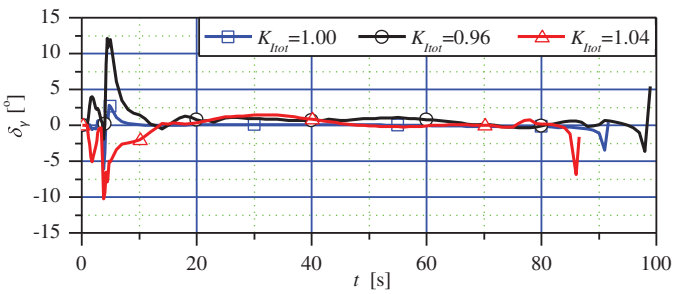


Figure 12. (Colour online) Fins deflection in the pitch.

The flight path angles, as a function of time, are given in Fig. 11 for three values of the total impulse corrective factors. The decrease of the flight path angles for the thrust greater than the nominal value is evident. For the thrust value lower than the nominal one, the increase of the flight path angles is required to hit the same target.

The diagrams of the control fin deflections in the pitch and yaw planes are given in Fig. 12. At the engine cut-off moment, the difference between the actual and nominal rocket velocity (Fig. 3) is evident. As a result, there is a sharp deflection of the fins in order to compensate for the differences between the actual and nominal velocity.

The values of the angles-of-attack and the sideslip angles are related to the control fin deflection. This relation is determined by the aerodynamic configuration of the rocket. The

https://doi.org/10.1017/aer.2016.4 Published online by Cambridge University Press

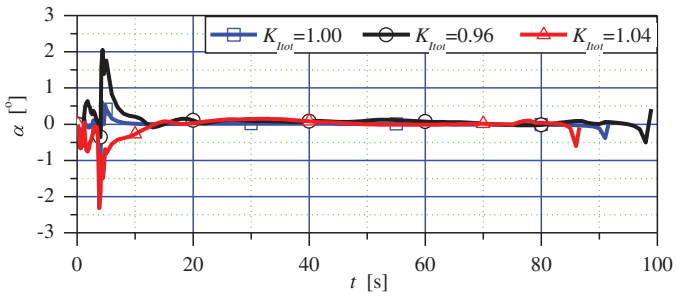


Figure 13. (Colour online) Angles-of-attack.

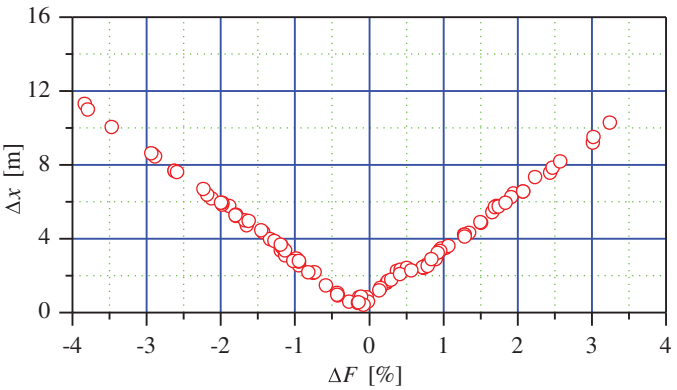


Figure 14. (Colour online) Absolute miss distance due to total impulse deviation.

diagrams of the angle-of-attack as a function of time are given in Fig. 13. The angle-of-attack is not greater than 5° in order to compensate for the maximum variation of the thrust (±4%).

The absolute values of the achieved range deviation as a function of the total impulse deviation for the guided artillery rocket are given in Fig. 14. It can be seen from the diagram that the maximum miss value is lower than 12 m.

5.0 MONTE CARLO ANALYSIS OF THE GUIDANCE SYSTEM ACCURACY

The specific forces $\mathbf{f}^b$ and the angular rates $\boldsymbol{\omega}_{ib}^b$ of the rockets are measured by accelerometers and rate gyros. The outputs of the accelerometers $\mathbf{f}_{\text{acc}}$ and the rate gyros $\boldsymbol{\omega}_{\text{r.g}}$ (Fig. 15) can be expressed mathematically in terms of the input values and the errors of measurements [9,10,15,16].

If the cross-coupling coefficients are neglected, a simplified mathematical model of measurements represents a function of the scale factor (**S**), the residual fixed bias (**B**), the random bias error (**n**) and the noise (**w**).

$$\mathbf{f}_{\text{acc}} = (\mathbf{I} + \mathbf{S}_{\text{acc}})\,\mathbf{f}^b + \mathbf{B}_{\text{acc}} + \mathbf{n}_{\text{acc}} + \mathbf{w}_{\text{acc}} \quad \ldots (40)$$

$$\mathbf{f}_{\text{acc}} = \mathbf{n}_{\text{acc}} + \mathbf{w}_{\text{acc}} \text{ for } |\mathbf{f}_{\text{acc}}| < |\mathbf{f}_{\text{d.b}}| \quad \ldots (41)$$

https://doi.org/10.1017/aer.2016.4 Published online by Cambridge University Press

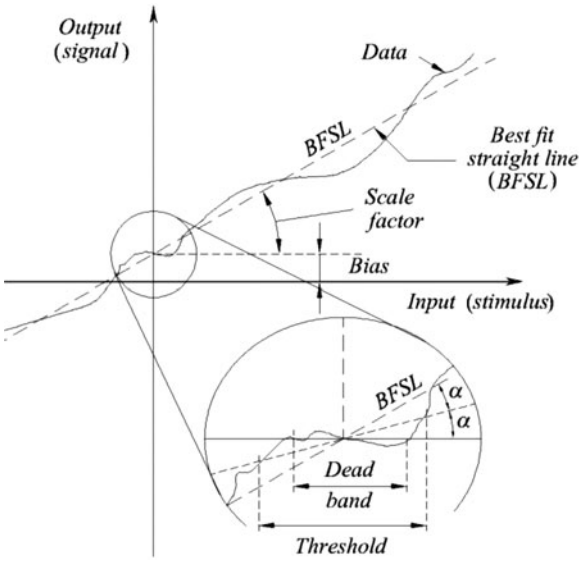


Figure 15. Measurement model.

$$\omega_{\mathrm{r.g}} = (\mathbf{I} + \mathbf{S}_{\mathrm{r.g}})\boldsymbol{\omega}_{ib}^{b} + \mathbf{B}_{\mathrm{r.g}} + \mathbf{n}_{\mathrm{r.g}} + \mathbf{w}_{\mathrm{r.g}} \quad \ldots (42)$$

$$\boldsymbol{\omega}_{\mathrm{r.g}} = \mathbf{n}_{\mathrm{r.g}} + \mathbf{w}_{\mathrm{r.g}} \quad \text{for} \quad \left|\boldsymbol{\omega}_{\mathrm{r.g}}\right| < \left|\mathbf{w}_{\mathrm{d.b}}\right|, \quad \ldots (43)$$

where $\mathbf{f}_{\mathrm{d.b}}$ is the dead band of accelerometers and $\mathbf{w}_{\mathrm{d.b}}$ is the dead band of rate gyros. For the compensated accelerometers and rate gyros, the residual fixed bias is equal to zero ($\mathbf{B}_{\mathrm{acc}} = 0$, $\mathbf{B}_{\mathrm{r.g}} = 0$).

The calculated values of the acceleration $\mathbf{f}_{\mathrm{acc}}$ and the angular rates $\boldsymbol{\omega}_{\mathrm{r.g}}$ must be included in the navigation algorithm in order to analyse the influence of the IMU measurement errors on the trajectory parameters' estimation. The specific force $\mathbf{f}^{b}$ (Equation (34)) and the angular rate in the body axis system $\boldsymbol{\omega}_{ib}^{b}$ (Equation (38)) are replaced by $\mathbf{f}_{\mathrm{acc}}$ and $\boldsymbol{\omega}_{\mathrm{r.g}}$, respectively.

$$\mathbf{f}^{s} = \mathbf{C}_{b}^{s}(\psi, \theta, \phi)\ \mathbf{f}_{\mathrm{acc}} \quad \ldots (44)$$

$$\boldsymbol{\omega}_{sb}^{b} = \boldsymbol{\omega}_{\mathrm{r.g}} - \mathbf{C}_{s}^{b}\left[\boldsymbol{\omega}_{ie}^{s} + \boldsymbol{\omega}_{0s}^{s}\right] \quad \ldots (45)$$

In order to verify the influence of the IMU accelerometers and the rate gyros measurement errors on the accuracy of the artillery rocket guidance system, a complex software program for numerical simulation has been built. It is composed of a 6DoF mathematical model of the missile flight, the SDINS navigation algorithm, a mathematical model of IMU measurement errors, a guidance system with a lateral acceleration autopilot and a CEP calculation of impact point dispersion by the Monte Carlo simulation.

The most dominant external disturbances (thrust deviation, thrust eccentricity and wind) are considered for the analysis of the guidance system accuracy:

- Variation of the thrust follows the normal Gaussian distribution law: $N(F_N, \sigma(F))$, where $\sigma(F)/F_N = 0.5\%$,

https://doi.org/10.1017/aer.2016.4 Published online by Cambridge University Press

Table 1
Parameters of the accelerometers and rate gyros measurements

	Accelerometer	Rate gyros
Scale factor	$s_{acc} = 0.1\ \%$	$s_{r.g} = 0.1\ \%$
Random bias instability	$n_{acc} = 0.2$ mg	$n_{rg} = 0.008\ ^\circ/s$
Noise	$\sigma_{acc} = 9.0$ mg	$\sigma_{rg} = 1\ ^\circ/\mathrm{s}$
Dead band	$f_{d.b} = 5.0$ mg	$\omega_{d.b} = 0.07\ ^\circ/s$

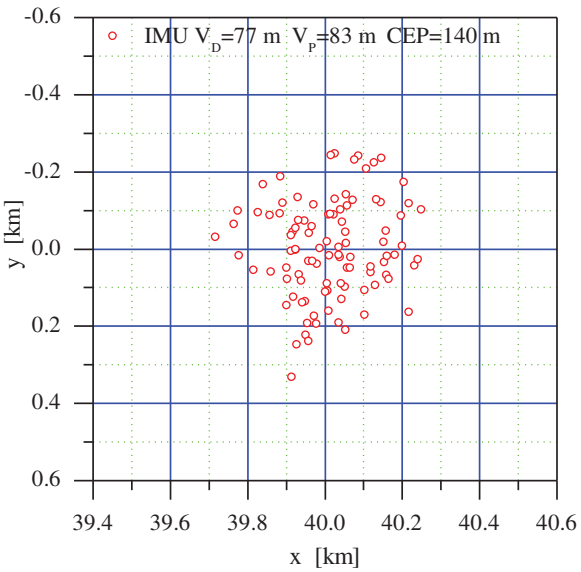


Figure 16. (Colour online) Impact point dispersion due to IMU measurement errors.

- Variation of the thrust eccentricity magnitude (ε_F) follows the normal Gaussian distribution law $N(0, \sigma(\varepsilon_F))$. A usual value of $\sigma(\varepsilon_F) = 1.0$ mrad. The angular position of the lateral thrust has the uniform distribution from 0 to 2π in the plane normal to the longitudinal axis $\varphi_{\varepsilon_F} = U(0,\ 2\pi)$,
- Axial and lateral winds have the normal distribution $N(0, \sigma_w)$ with zero mean values and the standard dispersion $\sigma_{w_x} = \sigma_{w_y} = 1.0$ m/s.

Without a loss of generality, the parameters of the accelerometers and rate gyros measurements[17] are the same for all three axes (Table 1).

It is shown that the flight path steering guidance system can compensate for all external disturbances without a miss at the target. In order to verify the influence of IMU measurement errors on the missile trajectory parameter estimation as well as on the guidance system accuracy, the numerical simulation of the guided ground-to-ground missile has been done with the IMU measurement error parameters, given in Table 1, without external disturbances. The impact point dispersion of the guided ground-to-ground missile at the range of 40.0 km with only the IMU measurement errors (Fig. 16) has been obtained by the Monte Carlo simulation of 100 trajectories.

https://doi.org/10.1017/aer.2016.4 Published online by Cambridge University Press

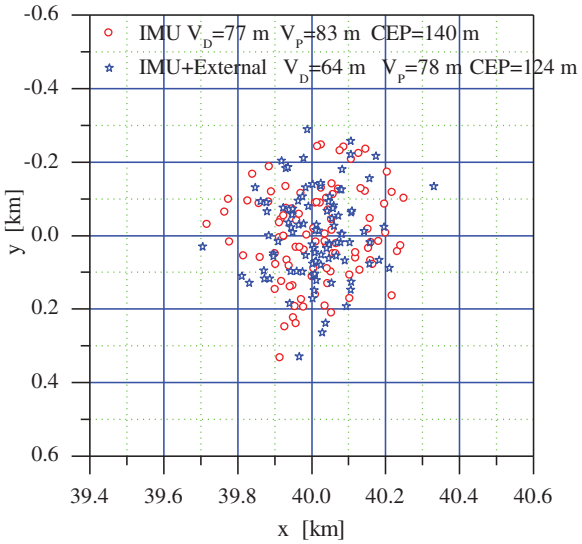


Figure 17. (Colour online) Impact point dispersion due to IMU measurement errors and external disturbances.

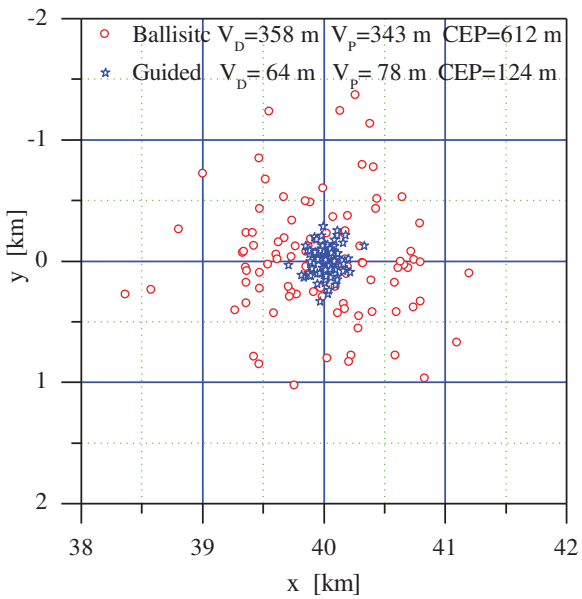


Figure 18. (Colour online) Impact point dispersion due to external disturbances.

When the external disturbances are included in the numerical simulation, the impact point dispersion is equal to the impact point dispersion due to the IMU measurement errors (Fig. 17).

The efficiency of the ground-to-ground missile guidance system with a typical commercial low-cost IMU is obtained by comparing the impact point dispersion of guided artillery rockets to the impact point dispersion of unguided rockets (Fig. 18). The external disturbances are the

https://doi.org/10.1017/aer.2016.4 Published online by Cambridge University Press

same in both cases. It is evident that guidance guided artillery rockets with commercial low-cost IMUs can decrease impact point dispersion by a factor of five compared to the dispersion of unguided artillery rockets.

6.0 CONCLUSION

The basic requirements for ground-to-ground rockets are increased range and accuracy. Both of these contradictory requirements can be met to some extent by using appropriate guidance and control systems. The guidance system based on the flight path steering method is used for trajectory correction. The flight path angle steering guidance algorithm requires the calculation of the nominal trajectory and the sensitivity coefficients at control points. The nominal trajectory is obtained by the numerical calculation of the ballistic flight of unguided rockets without disturbances. This trajectory and weighting factors at control points are calculated before the missile launch. The sampling interval of the control points has been chosen to fulfill the requirements that the position, velocity and sensitive coefficients between the control points can be obtained by linear interpolation.

The required (correlated) flight path angle is calculated by adding the correction to the nominal value of the flight path angle. To avoid normalisation of the time of flight to the values, the flight path angle is calculated as a function of the axial coordinate of the missile position. The correction of the flight path angle is a function of the difference between the actual trajectory and the nominal one in altitude, and the difference between the actual and nominal velocity. The flight path guidance system is realised with a synthetic pitch autopilot composed of an accelerometer and a rate gyro.

The efficiency of the flight path steering method developed in the paper has been verified for the artillery rocket with a maximum range of 50 km. The influence of the total impulse variation is verified by a numerical simulation for the achieved range of 40 km. The miss distance due to the 4% variation of the total impulse compared to the nominal value is 3 km. The guidance system added to the considered rockets and disturbances decreases the miss distance to 12 m. This relatively small miss distance is a result of the pitch rate in the feedback of the autopilot due to the influence of the gravity. The deflections of control fins are not equal to zero even for zero-demanded accelerations.

The strap-down navigation algorithm of the missile motion in the spherical axis system is used for trajectory estimation. The equation of missile motion in this axis system enables the determination of the trajectory parameters which can be used directly for the realisation of the flight path steering guidance system. Since the specific forces are measured by accelerometers and angular rates by rate gyros, the measurement errors are modelled as a function of the scale factor, bias instability, dead band and noise.

The efficiency of the artillery rockets with the flight path steering system has been analysed by a numerical simulation. There is no practical influence of external disturbances on the impact point dispersion. It is shown that IMU measurement errors are the dominant factor causing the impact point dispersion in guided artillery rockets. The influence of a typical commercial low-cost IMU has been analysed by the comparison of the impact point dispersion of unguided ballistic and guided artillery rockets. The required range and the external disturbances used for the numerical simulation are the same for both types of artillery rockets. It is shown that the impact point dispersion of guided artillery rockets with commercial low-cost IMUs decreased by a factor of five compared to the impact point dispersion of ballistic rockets.

https://doi.org/10.1017/aer.2016.4 Published online by Cambridge University Press

REFERENCES

1. GANTMAKHER, F.R. and LEVIN, L.M. *The Flight of Uncontrolled Rockets*, 1964, Pergamon Press Ltd, The Macmillan Company, NYC, New York, US.
2. GAMBLE, A.E. and JENKINS, P.N. Low cost guidance for the Multiple Launch Rocket System (MLRS) artillery rocket, *IEEE AES System Magazine*, January 2001.
3. HARKINS, T.E. and BROWN, T.G. Using active damping as a Precision Enhancing Technology for 2.75-Inch Rockets, U.S Army Research Lab, ARL TR-1772, 1999.
4. JITPRAPHAI, T. and COSTELLO, M. Dispersion reduction of a direct fire rocket using lateral pulse jets, *J of Spacecraft and Rockets*, 2001, **38**, (6), pp 929-936.
5. PAVKOVIC, B., PAVIC, M. and CUK, D. Q1 frequency-modulated pulse-jet control of an artillery rocket, *J of Spacecraft and Rockets*, 2012, **49**, (2), pp 286-294.
6. OLLERENSHAW, D. and COSTELLO, M. Model predictive control of a direct fire projectile equipped with canards, *J of Dynamic System, Measurement and Control*, November 2006, **130**, pp 061010-1-061010-12.
7. GREGORIOU, G. CEP calculation for a rocket with different control system, *J of Guidance*, May-June 1988, **11**, (3), pp 193-198.
8. SIOURIS, M.G. *Missile Guidance and Control Systems*, 2004, Springer-Verlag, NYC, New York, US.
9. ROGERS, R. *Applied Mathematics in Integrated Navigation System*, 2000, American Institute of Aeronautics and Astronautics, Inc, Reston, Virginia, US.
10. TITTERTON, D.H. and WESTON, J.L. *Strapdown Inertial Navigation Technology*, 2009, American Institute of Aeronautics and Astronautics, Inc, Reston, Virginia, US.
11. GARNEL, P. *Guided Weapon System*, 1980, Pergamon Press, NYC, New York, US.
12. BLAKELOCK, J.H., *Automatic Control of Aircraft and Missiles*, 1991, John Wiley and Sons, NYC, New York, US.
13. ĆUK, D. and MANDIĆ, S. Guidance and control laws design, *Theoretical Manual*, 2006, MTI, Belgrade, Serbia.
14. ĆUK, D., ĆURČIN, M. and MANDIĆ, S. Autopilot design, *Theoretical Manual*, 2004, MTI, Belgrade, Serbia.
15. IEEE Std 528-1994, IEEE Standard for Inertial Sensor Terminology, 1994, The Institute of Electrical and Electronics Engineers, New York, US.
16. IEEE Std 1293-1996, IEEE Standard Specification Format Guide and Test Procedure for Linear, Single-axis, Nongyroscopic Accelerometers, 1996, The Institute of Electrical and Electronics Engineers, New York, US.
17. Six Degrees of Freedom Inertial Sensor ADIS16360/16365, ANALOG DEVICES

https://doi.org/10.1017/aer.2016.4 Published online by Cambridge University Press